frontiers | Frontiers in Horticulture

TYPE Original Research
PUBLISHED 16 November 2022
DOI 10.3389/fhort.2022.1042105

OPEN ACCESS

EDITED BY
Aamir Raina,
Aligarh Muslim University, India

REVIEWED BY
Ayan Sadhukhan,
Indian Institute of Technology Jodhpur, India
Nasrin Moshtaghi,
Ferdowsi University of Mashhad, Iran

*CORRESPONDENCE
Fadi Chen
chenfd@njau.edu.cn

SPECIALTY SECTION
This article was submitted to Breeding and Genetics, a section of the journal Frontiers in Horticulture

RECEIVED 12 September 2022
ACCEPTED 31 October 2022
PUBLISHED 16 November 2022

CITATION
Gao R, Wang H, Qi X, Zhu L, Yang X, Chen S, Jiang J, Wang Z and Chen F (2022) ClNAC84 interacts with ClMIP to regulate the cell cycle and reduce the size of *Chrysanthemum lavandulifolium* organs. *Front. Hortic.* 1:1042105. doi: 10.3389/fhort.2022.1042105

ClNAC84 interacts with ClMIP to regulate the cell cycle and reduce the size of *Chrysanthemum lavandulifolium* organs

Ri Gao[1,2], Haibin Wang[1], Xiangyu Qi[1], Lu Zhu[1], Xiaodong Yang[1], Sumei Chen[1], Jiafu Jiang[1], Zhenxing Wang[1] and Fadi Chen[1]*

[1]State Key Laboratory of Crop Genetics and Germplasm Enhancement, Key Laboratory of Landscaping, Ministry of Agriculture and Rural Affairs. Key Laboratory of Biology of Ornamental Plants in East China, National Forestry and Grassland Administration, College of Horticulture, Nanjing Agricultural University, Nanjing, China, [2]College of Agricultural, Yanbian University, Yanji, Jilin, China

The *NAC* transcription factor is plant-specific proteins and one of the largest families of transcription factors in plants. NAC proteins are involved in various aspects of plant growth and development, but little is known about how NAC proteins regulate the cell cycle. Here, we characterized ClNAC84 from *C. lavandulifolium* (an NAC transcription factor). *ClNAC84* overexpression in *C. lavandulifolium* resulted in a semi-dwarf phenotype with shorter plant height, smaller leaf size, and smaller flower size than wild-type plants. The number of cells in the S phase during the cell cycle was less in *ClNAC84*-overexpression transgenic *C. lavandulifolium* than in wild-type *C. lavandulifolium*. This indicates that *ClNAC84* overexpression can induce cell cycle arrest at the S and G2 phases. To elucidate the *ClNAC84* regulatory network, ClMIP protein was shown to interact with ClNAC84 *in vitro* and *in vivo*. *ClMIP* overexpression in *C. lavandulifolium* also resulted in dwarfism and decreased cell numbers, and the expression level of *ClKRP5* was higher in transgenic *C. lavandulifolium* than in wild-type plants. We also found that ClMIP can bind to the promoter of *ClKRP5*. Our data indicate that the interaction between ClNAC84 and ClMIP may promote *ClKRP5* expression and inhibit S and G2 phases of the cell cycling.

KEYWORDS

***Chrysanthemum lavandulifolium*, ClNAC84, ClMIP, cell cycle, ClKRP5**

Introduction

Cell growth and division are essential processes in plant growth and development (Grandjean, 2004). The cell cycle includes the G1, S, and G2 phases which are affected by multiple genes including some cell division related genes (PBR-binding protein *E2F*, KIP-related proteins *KRPs*, cyclins *CYCs* and cyclin-dependent kinases *CDKs*) and some transcription factors such as *NAC* and v-myb avian myeloblastosis viral oncogene homolog (*MYB*), with the transcription factor NAC playing an important role. NAC (NAM, ATAF1/2, and CUC2) proteins are plant-specific transcription factors. The *NAC* genes are NO APICAL MERISTEM (NAM) and CUP-SHAPED-COTYLEDON 1 (*CUC1*), *CUC2*, and *CUC3* in *Petunia* and *Arabidopsis*, respectively, all of which regulate the shoot apical meristem (Souer et al., 1996; Aida et al., 1997). Rice, *Arabidopsis* (Ooka et al., 2003), and *Chrysanthemum* (Huang et al., 2012) comprise 161, 138, and 44 NAC members, respectively, which are further classified into 6–18 subfamilies and are involved in regulating various biological processes involved in plant growth and development. A typical *NAC* transcription factor has a highly conserved NAC domain and a transcriptional regulatory (TR) region in their N-terminal and C-terminal regions, respectively. The NAC domain is further divided into five subdomains (A-E). Subdomain A is involved in the formation of a functional dimer, subdomains B and E make up the functional diversity of the NAC protein, and the highly conserved subdomains C and D can bind to DNA (Puranik et al., 2012). In addition, in rice, NAC proteins are divided into 15 types (A-O) according to the motifs: A-E contain NAC domain and transcriptional regulatory regions as the typical motifs, and the other types include NAC-like proteins as the distinct motifs (Fang et al., 2008).

The phenotype of a double mutant *namcuc* showed a fusion of cotyledons, flowers, floral organs, and ovules that formed a "cup" in *Arabidopsis* (Aida et al., 1997) through the restraining behaviors of boundary cells that block the fusion of organs (Aida and Tasaka, 2006). PIN-FORMED1 (*PIN1*) encoding the auxin efflux carrier was regulated by MONOPTEROS (*MP*) genes, and the corresponding mutants showed cotyledon fusion or defects in apical patterning and perturbations in embryo development, a process controlled by *CUC* genes (Aida et al., 2002), implying that *CUC* genes could respond to auxin signals. In addition, *CUC* can affect leaf morphology. In *Arabidopsis*, TCP (Teosinte branched1/cincinnata/proliferating cell factor) protein can interfere with the function of miR164 and CUC proteins, preventing the formation of serrated leaves at the seeding stage. In the aging pathway of plants, the accumulation of *SPL* mRNA is gradual. SPLs bind to TCP protein and reduce the formation of complex TCP and CUC. This instability causes activation of CUC protein complexes, increasing the complexity of leaf morphology (Rubio-Somoza et al., 2014). A similar phenomenon was also reported in tomatoes; atypical type II phosphatidylinositol 4-kinase (PI4KII) interacts with ANAC078 to suppress auxin synthesis and inhibit the formation of serrated leaves (Tang et al., 2016). NAC proteins not only regulate the development of cotyledons and leaf organs but also regulate plant height. The leaf size and plant height of *ANAC036*-overexpression transgenic plants were smaller than wild-type (WT) plants with a semi-dwarf phenotype. *ANAC036* overexpression in rice resulted in smaller cell sizes in transgenic plant leaves than in WT plant leaves (Kato et al., 2010). XYLEM NAC DOMAIN1 (*XND1*) of NAC domain transcription factor members is mainly expressed in the plant xylem, and in plants overexpressing *XND1*, it reduced the number of tracheary elements compared to that in WT plants. Transmission electron microscopy showed that the secondary wall of parenchyma cells in transgenic plants did not develop well in the hypocotyls (Zhao et al., 2008). *NTM*, a membrane-bound *NAC* transcription factor, participates in the regulation of intramembrane proteolysis and mediates cytokine signaling during cell division. The *Arabidopsis* mutant *ntm* shows serrated leaves and dwarfism in plants with a significant reduction in the expression levels of histone *H4* and *CDK* and an increase in the expression levels of *CDK* inhibitor genes (KIP-related proteins) (Kim et al., 2006). Willemsen et al. (2008) reported that the transcription factors *FEZ* and *SMB* (Sombrero) containing the NAC domain also regulate the orientation and timing of cell division in *Arabidopsis* stem cells. These data show that members of the NAC family are involved in cell cycle regulation in plants. The correlation between the changes in the G1, S, and G2 phases and NAC proteins, however, remains elusive.

Tetraploid *C. lavandulifolium* (Fisch. ex Trautv.) flowers are larger than diploid flowers because of enhanced cell numbers. A previous study in which the NAC fragment was screened by cDNA-AFLP and *ClNAC84* was cloned showed that these may be involved in cell cycle regulation (Gao et al., 2016). In this study, we report that the *ClNAC84* transcription factor gene from *C. lavandulifolium* plays a role in the cell cycle and the ClMIP protein potentially interacts with ClNAN84, which activates *ClKRP5* by binding to its promoter resulting in inhibition of the cell cycle S and G2 phases.

Materials and methods

Plant materials and growth conditions

C. lavandulifolium for *ClNAC84* cloning and expression analysis and transgenic lines were maintained by the Chrysanthemum Germplasm Resource Preserving Center, Nanjing Agricultural University, Nanjing, China. The plants were potted in a 1:1 (v/v) mixture of soil and vermiculite and

grown in a greenhouse at day/night temperatures of 24°C/18°C and an 8/16 h light/dark photoperiod with a relative humidity of 70%.

Isolation of ClNAC84

Total RNA was extracted from the stem apex of *C. lavandulifolium* seedlings using RNAiso reagent (TaKaRa, Tokyo, Japan) according to the manufacturer's instructions. Based on *C. nankingense* expressed sequence tags (Wang et al., 2013), ClNAC84-fF/fR primers (Table S1) were designed to amplify full-length *ClNAC84* by rapid amplification of cDNA ends (RACE) PCR. The resulting PCR product was purified and cloned into T-Vector pMD19 (Simple) (TaKaRa) for sequencing. The *ClNAC84* amino acid sequence was aligned with those of other plant homologs using BLAST (http://www.ncbi.nlm.gov/blast) and DNAMAN 5.2.2. Phylogenetic trees were constructed using the neighbor-joining method and MEGA (version 5.0). Internal branching support was estimated using 1000 bootstrap replicates.

Subcellular localization

The *ClNAC84* ORF containing *BamH*I and *Not*I sites and the pENTR^{TM}1A dual selection vector (Invitrogen) were digested (*BamH*I and *Not*I), ligated to generate a set of pENTR^{TM}1A-*ClNAC84* fusions, and then subcloned into the pMDC43 vector with GFP for transient expression in onion epidermal cells (ClNAC84-pF/pR primer sequence in Table S1). After incubation for 20 h at 25°C in the dark, GFP expression was observed in onion epidermal cells *via* confocal laser microscopy (LeicaSP2, Germany).

Yeast transformation, growth, and observation

The coding region of *ClNAC84* was inserted into the expression vector pESPM with T_4 DNA ligase after double enzyme restriction (*Xho*I and *Sal*I). The pESPM-ClNAC84 plasmid was transformed into the fission yeast strain *SPQ-01* (Leu^-) according to the manufacturer's transformation system 2 (TaKaRa). Cells were selected on Edinburgh Minimal Medium (EMM) with thiamine at 30°C. Yeast containing the pESPM empty vector was used as a control. The yeast was cultured in liquid EMM medium to the logarithmic phase stage, washed three times with EMM liquid medium to remove the thiamine for de-repressing the NMT1 promoter, which drives *ClNAC84* expression; and cultured at 30°C for 20 h. Total RNA was isolated from pESPM-NAC84 overexpressing yeast strains selected on EMM medium with and without thiamine, using the yeast RNAiso Kit (TaKaRa). First-strand cDNA was synthesized from 1 μg of total RNA using M-MLV reverse transcriptase (TaKaRa). Gene-specific primers ClNAC84-oF/R were designed to amplify the transcripts, and *tubulin* was used as the reference gene (Table S1). PCR amplification was initially denatured (94°C for 4 min), followed by 29 cycles at 95°C for 30 s, 57°C for 30 s, and 72°C for 45 s. The transformed mid-exponential yeast cells (OD_{600} = 0.5) at 1-, 10-, 100-, and 1000-fold dilutions were inoculated on EMM media plates with or without thiamine, followed by incubation at 30°C for 60 h. To observe the cell density and shape, the yeast cells were fixed with 70% ethanol alcohol for 30 min, and to examine the DNA, the cells were stained with DAPI (1 mg/ml) and observed under a fluorescence microscope (Olympus Optical Co., Ltd).

Morphological investigation of transgenic *C. lavandulifolium*

To further investigate the functions of *ClNAC84* and *ClMIP*, pMDC43-*ClNAC84* and pMDC43-*ClMIP* were constructed and transformed into *Agrobacterium tumefaciens* strain *EHA105* by the freeze-thaw method. Genetic transformation of *C. lavandulifolium* was performed according to the methods in a previous study (Gao et al., 2018). Each line was repeated 10 times, and the data are presented as the mean ± standard error. SPSS v17.0, and Microsoft Excel 2016 were used for the statistical analysis ($p < 0.05$).

Transcriptional activity analysis

ClNAC84 transcriptional activity assays were performed using the Match maker GAL4 One-Hybrid System (Clontech, Mountain View, CA, USA). The pGBKT7-*ClNAC84* vector was constructed and introduced into yeast strain Y2HGold (Clontech) following the manufacturer's protocol, and the empty pCL1 and pGBKT7 vectors were transformed into the yeast strain as positive and negative controls, respectively. pGBKT7-*ClNAC84* and pGBKT7 were cultured on SD medium without tryptophan (SD/-Trp), while the pCL1 transformants were incubated on SD medium without leucine (SD/-Leu). After culturing at 30°C for 3 d, the transgenic cell lines were transferred onto SD medium lacking both histidine and adenine (hemisulfate salt) either in the presence or absence of β-galactosidase.

Y2H assay

Protein–protein interaction Y2H assays was performed using a GAL4-based Y2H system (Matchmaker Gold Systems; Clontech, Palo Alto, CA, USA). The full-length coding sequence

of the candidate gene *ClMIP* was inserted into pGBKT7 (Clontech, Mountain View, CA, USA). The ClMIP-gF/gR primers were used to create the constructs and are listed in Table S1. The bait and prey plasmids were co-transformed into the yeast strain Y2HGold (Clontech, Palo Alto, CA, USA). Yeast transformation was performed according to the manufacturer's instructions. The co-transformants were incubated in SD medium lacking Leu, Trp, His, and Ade (SD/-Leu/-Trp/-His/-Ade/+X-α-Gal) plates, after culturing at 30°C for 3 days to obtain a graph.

Bimolecular fluorescence complementation assay

The BiFC assay was used to study the interaction between *ClNAC84* and *ClMIP*. To construct pSAT4A-*ClNAC84*-nEYFP-N1 and pSAT4A-*ClMIP*-cEYFP-N1 vectors, *ClNAC84* and *ClMIP* ORF were amplified using ClNAC84-bF/R and ClMIP-bF/bR primers (Table S1); recombined with the N- and C-termini of YFP, respectively; and subsequently introduced into the pSAT4A vector. The two plasmids were mixed with gold particles and transformed as described above for transient expression analysis. Confocal laser microscopy was used to monitor the expression of YFP.

ClKRP5 promoter cloning and vector construction

Genomic DNA was isolated from *C. lavandulifolium* using the Plant Genomic DNA Rapid Extraction Kit (TaKaRa, Beijing, China). According to the *ClKRP5* full-length cDNA, ClKRP5-fF/fR primers were designed to amplify intron-containing regions. The promoter region of *ClKRP5* was amplified from the genomic DNA, purified, and cloned into the T-Vector pMD19 (Simple) (TaKaRa) for sequencing using the improved TAIL-PCR method (Li et al., 2015). Briefly, based on the genomic sequence of *ClKRP5*, three gene-specific primers (GSP1, GSP2, and GSP3) were designed, and the other four primers AP1, AP2, AP3, and AP4 were from the TaKaRa kit (Table S1). PCR conditions and procedures were performed according to the manufacturer's instructions. The final PCR-amplified products (>1000 bp) were purified and cloned into the T-Vector pMD19 (Simple) (TaKaRa) for sequencing.

The *ClKRP5* promoter (1479 bp) was amplified using LA Taq (TaKaRa) with the primer pair KRP5-pF/R containing *Bam*H I and *Hind* III sites (Table S1). The PCR products were subcloned into the pMD19-T vector and confirmed by sequencing. pMD19-T harboring *ClKRP5* and pCAMBIA1381Z were digested with *Bam*H I and *Hind* III, respectively. The purified products were ligated with T_4 DNA ligase to obtain the vector pCAMBIA1381Z-KRP*pro*.

DNA-binding assay of CmKRP5 using a yeast one-hybrid system

To examine whether *ClMIP* has DNA-binding ability to the *ClKRP5* promoter, a yeast one-hybrid assay was performed using a Clontech system (Clontech, Mountain View, CA, USA). The *ClKRP5* promoter sequence was constructed into a pHIS expression vector, and both pGADT7-*ClMIP* and pHIS-*ClKRP5pro* were transfected into the yeast strain Y1H (Clontech). The empty vectors pGADT7 and pHIS-*ClKRP5pro* were used as negative controls. The growth status of the transformed yeast cells was tested on SD/-His-Ura-Leu medium containing 50 mM 3-AT. The culture conditions were the same as those for the Y2H assay.

Split-LUC assay

The constructs were transformed into *Agrobacterium* strain 1301 with 35S::p19 and used to co-infiltrate 3-week-old tobacco leaves as follows: pCAMBIA1381Z-*ClKRP5pro*, pMDC43-*ClNAC84*, pCAMBIA1381Z-*ClKRP5pro* + pMDC43-*ClNAC84*, pCAMBIA1381Z-*ClKRP5pro* + pMDC43-*ClMIP*, and pCAMBIA1381Z-*ClKRP5pro* + pMDC43-ClMIP + pMDC43-*ClNAC84*. The infiltrated tobacco plants were grown for an additional 3 days in a growth chamber under a 16/8 h light/dark photoperiod at 21°C. LUC images were captured using a low-light cooled CCD imaging apparatus (DU934P Andor, UK). LUC activity was measured with 10 s integration periods (Promega, Madison, Wisconsin, USA). Counts of luminescence were quantified using a $20/20^n$ luminometer (Turner BioSystems). Three independent experiments were performed for each assay.

Flow cytometric analysis

The *ClNAC84* or *ClMIP* overexpression and WT *C. lavandulifolium* leaves were cultured on MS medium containing 6-benzylaminopurine 1.5 mg L^{-1} and naphthaleneacetic acid 0.8 mg L^{-1} for callus induction. Cells from the callus culture were resuspended in the above medium. This synchronous cell culture method was based on that of Menges (Menges and Murray, 2002). The synchronous cells were filtered with nylon mesh (pore size 300 mesh) and collected in microcentrifuge tubes (100 mmol L^{-1} citric acid monohydrate; 5 μg L^{-1} RNase; 0.5% (v) Tween20; pH 2.0–3.0) and stained with propidium iodide. The samples were then incubated at 4°C in an icebox for 30 min after flow cytometry analysis (Coulter Epics XL, Beckman Coulter, Miami, USA). The percentage of cells in different cell cycle phases was evaluated using ModfidLT4.1 program. The experiments were repeated at least ten times

using independent apical bud samples. The data were evaluated by Student's t-test (one-tailed distribution, two-sample equal variance) using SPSS v16.0 (SPSS, Inc., Chicago, IL, USA). The data were considered significant at $p < 0.05$.

qRT-PCR *analysis*

Total RNA was isolated from the different tissues of *C. lavandulifolium* various developmental periods by using RNAiso (TaKaRa) in accordance with the manufacturer's instructions. cDNA was synthesized from 1000 ng of total RNA by using a reverse transcriptase FastQuant RT kit (Tiangeng). Gene-specific primers were designed for the 3′UTR sequences, and elongation factor 1a (*ClEF1α*) was used as the reference sequence (Table S1). Three replicates of qRT-PCR data were processed using the comparative CT method (Gao et al., 2018).

Results

Characterization of ClNAC84

The *ClNAC84* sequence isolated from the cDNA of *C. lavandulifolium* contains an open reading frame (ORF) of 690 bp and encodes a protein of 229 amino acids. A BLASTP search showed that the deduced polypeptide is similar to NAC proteins from a range of plant species and contains a highly conserved NAC domain (a, b, c, d, and e) in the N-terminus and a transcriptional regulation domain (f) in the C terminus (Figure 1A). To investigate the potential role of *ClNAC84* in regulating plant development, we evaluated its expression in different organs, including apical buds, flower buds, leaves, stems, and roots at different developmental stages. *ClNAC84* transcripts were detected in all the investigated organs. Relative transcript abundance in different organs gradually decreased from young plants to the full flowering stage, but transcript abundance in flower buds increased at visible capitulum stages and then declined at the full flowering stage. Transcript abundance in apical buds and leaves of young plants was significantly higher than that in other organs at various stages of development (Figure 1B). These results suggest that during plant development, *ClNAC84* was expressed at high levels in the apical buds and flower buds.

The green fluorescent protein (*GFP*)-*ClNAC84* fusion construct under the control of the 35S promoter was used to investigate the subcellular localization of ClNAC84. In onion epidermal cells, green fluorescence of *35S::GFP-ClNAC84* markedly accumulated in the nucleus, while the product of the control *35S::GFP* transgene was deposited throughout the onion epidermal cells (Figure 1D). Next, we performed a transcription activation assay using yeast. The harboring the complete GAL4 domain (pCL1) and pGBK7 vector were used as positive and negative controls, respectively. Yeasts harboring *ClNAC84* were not able to activate the reporter genes His, Leu, and X-α-Gal (Figure 1C). The results showed that ClNCA84 had no transcriptional activation activity in yeast cells.

ClNAC84 overexpression suppressed *C. lavandulifolium* growth by inhibition of cell cycle

To investigate the function of *ClNAC84*, *ClNAC84* was overexpressed in *C. lavandulifolium* (OX), and six transgenic lines were obtained; the presence of the gene was confirmed by PCR. The OX-7, OX-12, and OX-13 lines, which had the highest levels of *ClNAC84* expression, were selected for further investigation (Figure S1). Morphological changes, such as changes in plant height, leaf length, leaf width, leaf area, inflorescence diameter, flower disk diameter, ligulate flower length, number of ligulate florets, and tubular flower length, were observed in each transgenic plant. Only the ligulate flower number showed no obvious differences compared with that in the WT plants (Figure 2A (a–j), Table 1).

Because the leaves of overexpression lines were thinner and smaller than those of WT plants, we observed the anatomical structure of the leaves and found that the palisade tissue thickness decreased by 14.89%, while the upper and lower epidermis thickness and spongy tissue thickness showed little change (Figure 2A (h–k), Table 2). To further understand the effect of *ClNAC84* overexpression on *C. lavandulifolium* leaf development, epidermal cells of the leaves of overexpression lines and WT *C. lavandulifolium* were inspected using differential interference contrast microscopy. The number of palisade cells was significantly changed in the leaves of transgenic plants but decreased by 26.1% in overexpression lines; the cell size showed no change. These data indicated that the leaves of overexpression lines became smaller through the retardation of cell division (Figure 2A (i–l), Table 2).

To further reveal the potential role of *ClNAC84* in cell division, we investigated the function of *ClNAC84* in the yeast system. The NMT promoter in the pESPM vector drives gene expression in the absence of thiamine (-VB1); it also inhibits gene expression in the presence of thiamine (+VB1) (Mu et al., 2009). The transformants harboring *ClNAC84* showed higher expression levels under -VB1 than under +VB1 (Figure S2A). Under inductive conditions (-VB1), the proliferation of transformants harboring *ClNAC84* was inhibited in comparison with that of transformants harboring the control vector. Under surpressive conditions (+VB1), there was no difference in proliferation between transformants harboring *ClNAC84* and those harboring the control vector (Figure S2B). The yeast transformants in the liquid medium under -VB1 were stained with 4,6-diamidino-2-phenylindole (DAPI) and

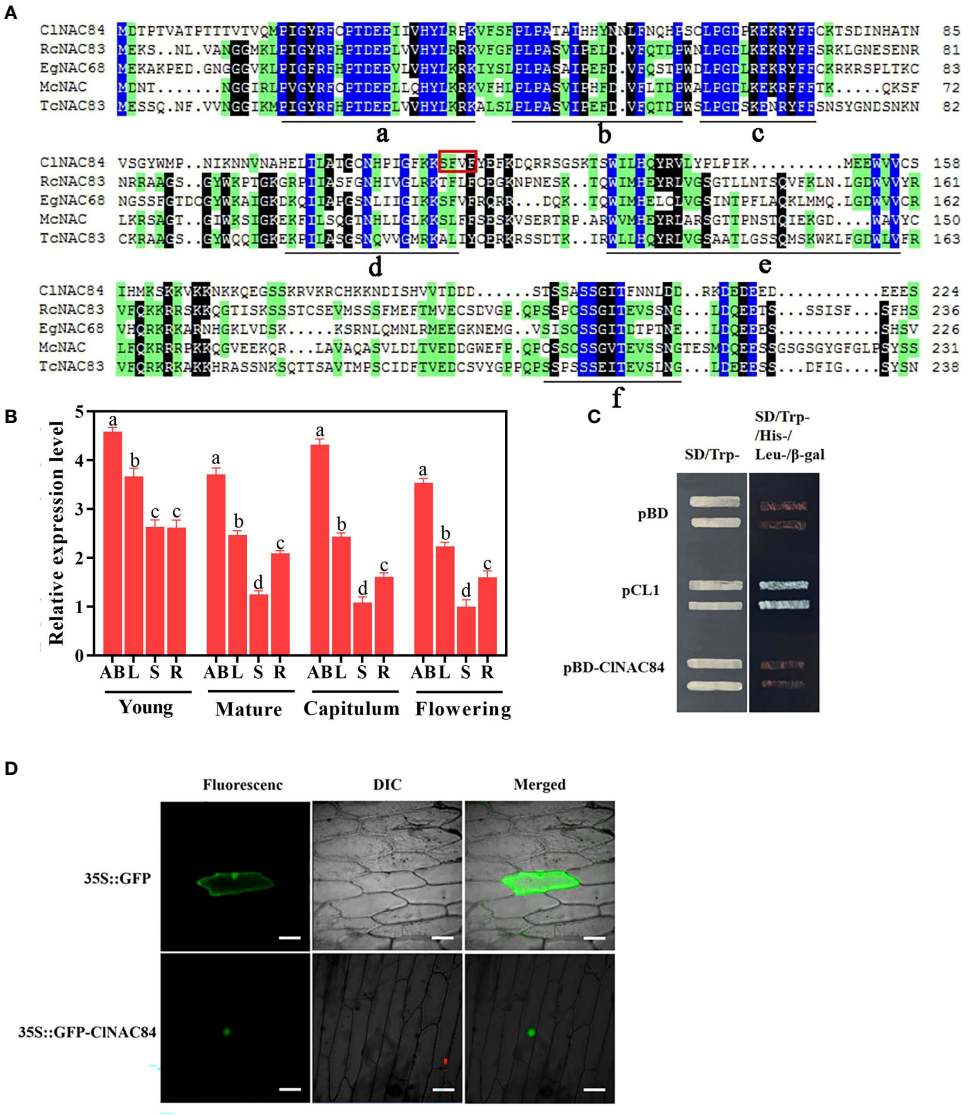

FIGURE 1
Characterization of *ClNAC84*.**(A)** The deduced amino acid sequence of *ClNAC84* and other genes harboring a NAC domain. The NAC domain (a, b, c, d, e) and transcriptional regulation domain (f) are shown underlined. The GenBank accession numbers of the referred to genes are as follows: *RcNAC83* (XP_002512886.1), *EgNAC68* (XP_012844037.1), *McNAC* (AKO82482.1), *TcNAC83* (XP_007031956.2). **(B)** *ClNAC84* expression in different tissues at various developmental periods: young, young plant (height 20 cm); mature, mature plant before flower differentiation; capitulum, visible capitulum; flowering, full flowering; AB, apical buds; L, third leaves; S, stems of between third leaves and second leaves; R, roots; FB, flower buds. Uppercase letter represents significant differences in the analyses of apical (flower) buds at various developmental stages; lowercase letter indicates between the leaves. Error bars indicate SE (n = 3). Significant differences were analyzed by Tukey multiple range test ($p < 0.05$). **(C)** Transcriptional activation in yeast. pCL1 and pBD plasmids (pGBKT7) represent, respectively, the positive and negative controls. Left: SD medium lacking tryptophan; right: SD medium lacking tryptophan, histidine, and leucine and supplemented with β-Gal. **(D)** Subcellular localization of *ClNAC84* transiently expressed by the *35S::GFP-ClNAC84* transgene in onion epidermal cells. Left: dark field image, center: bright field image, right: merged image. *35S::GFP* transgene was used as a control. Bar: 50 μm.

observed under a fluorescence microscope. The cell morphology showed no difference between yeast cells containing *ClNAC84* and those containing the pESPM vector. However, the percentage of yeast cells containing double nuclei was 5.2 times more in *ClNAC84* cells than in pESPM cells (Figure S2C). In the yeast cell growth curve analysis, cell density (OD = 600) of the yeast cells containing *ClNAC84* was consistently lower than that of yeast cells containing the pESPM vector in the -VB1 liquid medium after 4 h of culture; significant differences were noted in cell density 6 h later (Figure S2D). These results indicate that *ClNAC84* decreases the proliferation of yeast cells and promotes the occurrence of double nuclei.

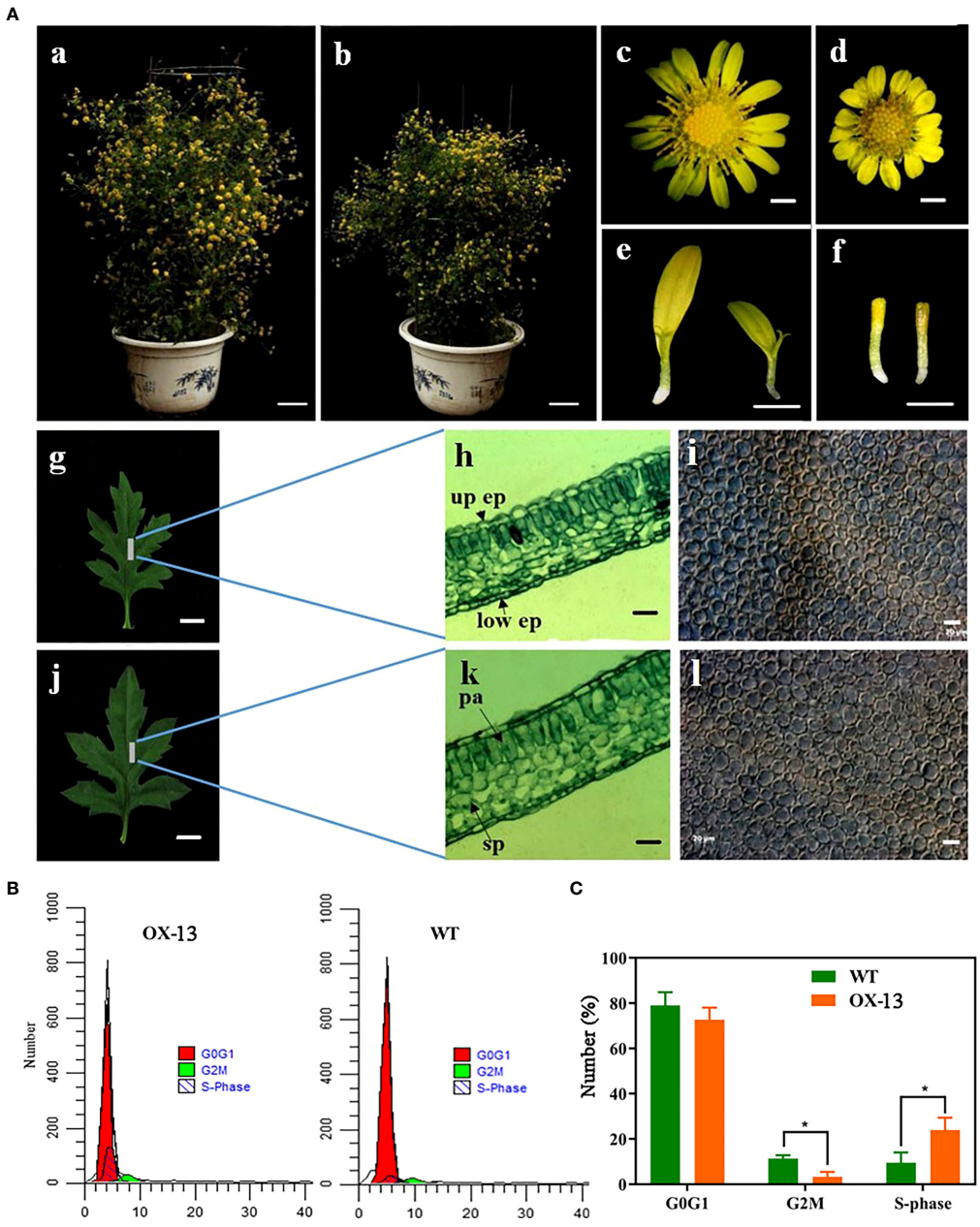

FIGURE 2
ClNAC84 overexpression suppressed *C. lavandulifolium* growth by inhibition of cell cycle. **(A)** Phenotypic characterization of ClNAC84 overexpression *C. lavandulifolium*. (a, c, g, h, and i) Wild-type *C. lavandulifolium*, flower, leaf, anatomical structure of leaf, and cells of palisade tissue first layer. (b, d, j, k, and l) *ClNAC84*-overexpressing plant (OX-13), flower, leaf, anatomical structure of leaf, and cells of palisade tissue first layer. (e) ligulate florets of wild-type plant (left) and *ClNAC84*-overexpressing plant (right). (f) tubular florets of wild-type plant (left) and *ClNAC84*-overexpressing plant (right). (h and k) up ep, upper epidermis; low ep, lower epidermis; sp, spongy tissue; pa, palisade tissue. (a and b) bars = 5 cm; (c, d, e, and f) bars = 2 mm; (g and j) bars = 5 mm; (h, k, i, and k) bars = 20 μm. **(B)** Comparison of the flow cytometric profiles of wild-type and *ClNAC84* overexpression *C. lavandulifolium*. Red peaks indicate normal G0G1 cell number, green peaks indicate G2M cell number, and black peaks indicate S phase cell number. **(C)** The cell number at different phases of the cell cycle. The percentages were derived from **(B)**.

To further determine whether the phase of the cell cycle was blocked in *C. lavandulifolium* overexpressing *ClNAC84*, we collected synchronous cells of OX-13 lines and WT plants for cell cycle analysis. The number of S stage cells in *ClNAC84* overexpression lines was more than twice that of the WT plants, but the number of G2M stage cells from WT plants was 3.28% lower than that of overexpression lines (Figures 2B, C). These results indicate inhibition of the cell cycle.

10.3389/fhort.2022.1042105

TABLE 1 Morphology of wild type and transgenic overexpressing *ClNAC84 C.lavandulifolium*..

Characters	WT	OX-7	OX-12	OX-13
Plant height (cm)	82.22 ± 0.85a	73.29 ± 0.76b	75.66 ± 0.66b	76.55 ± 1.17b
Leaf length (cm)	4.32 ± 0.06a	3.17 ± 0.14b	2.92 ± 0.06b	3.37 ± 0.07b
Leaf width (cm)	2.83 ± 0.06a	2.23 ± 0.08b	1.94 ± 0.10b	2.03 ± 0.16b
Leaf area (mm^2)	392.41 ± 13.07a	274.37 ± 7.25b	283.34 ± 12.38b	304.17 ± 14.58b
Inflorescence diameter (mm)	17.02 ± 0.18a	12.83 ± 0.37b	13.57 ± 0.25b	13.47 ± 0.39b
Flower disc diameter (mm)	8.03 ± 0.12a	5.75 ± 0.18b	6.48 ± 0.24b	6.75 ± 0.36b
No. of ligulate florets	15.93 ± 0.18a	16.56 ± 0.36a	17.23 ± 0.19a	16.47 ± 0.17a
Ligulate flower length (mm)	7.57 ± 0.08a	5.05 ± 0.24b	5.23 ± 0.096b	5.32 ± 0.18b
No. of tubular florets	85.34 ± 1.244a	74.49 ± 1.46b	73.60 ± 1.28b	70.79 ± 0.94b
Tubular flower length (mm)	4.18 ± 0.15a	3.43 ± 0.13b	3.55 ± 0.15b	3.57 ± 0.12b

Data are presented as mean ± standard error. Letters indicate significant differences at p = 0.05 by Tukey's test.

ClNAC84 interacts with ClMIP

To elucidate the mechanism of *ClNAC84* in cell division, we identified cell division-related proteins including ClMIP, ClH2B1, and ClMafB transcription factors by screening the yeast library (Table S2). ClMIP is known as ClAE or FAM96 (family with sequence similarity 96, member B). To assess whether ClNAC84 and ClMIP proteins interact, we performed yeast two-hybrid (Y2H) assays. ClNAC84 grew well and appeared as a blue spot when co-transformed with ClMIP, and the positive control exhibited X-α-Gal activity, but the negative control did not (Figure 3A). Bimolecular fluorescence complementation (BiFC) experiments showed that a yellow fluorescent protein (YFP) signal was observed in onion epidermis cells co-expressing nEYFP-*ClNAC84* and cEYFP-*ClMIP*. In contrast, there was no YFP signal in cells co-expressing nEYFP-*ClNAC84* and cEYFP or nEYFP and in cEYFP-*ClMIP* as controls (Figure 3B). These results demonstrate that ClNCA84 interacts with ClMIP in plant cells.

Involvement of ClMIP in the regulation of cell cycle

To further clarify the function of *ClMIP*, the *35S::ClMIP* vector was transformed into *C. lavandulifolium*, and three transgenic lines, OX-m1, OX-m2, and OX-m3, were obtained after qRT-PCR identification (Figure S3). Differences in phenotypes were observed between transgenic and WT plants. The plant height, leaf length and width, leaf area, inflorescence, flower disk diameter, tubular flower number, and tubular flower length of transgenic plants were less than those of WT plants (Figure 4A a–e, Table 3). Epidermal cell area and number decreased by 15.51% and 20.29%, respectively, in the transgenic lines (Figure 4A, f, g, Table 3). We investigated the number of G0G1, S, and G2M phase cells of WT and OX-m3 by flow cytometry. The number of S phase cells in OX-m3 was 33.29% higher than that in WT plants, and the number of G0G1 and G2M phase cells was higher in WT plants than in OX-m3 (Figures 4B, C).

TABLE 2 Anatomy of leaf tissues from WT and overexpressing *ClNAC84* plants.

Anatomy	WT	OX7	OX12	OX13
Palisade thickness(μm)	43.39 ± 0.19a	36.68 ± 0.60b	37.11 ± 0.47b	37.00 ± 0.66b
Spongy tissue thickness (μm)	76.67 ± 0.58a	75.58 ± 0.60a	78.79 ± 0.69a	77.94 ± 0.93a
Upper epidermis thickness (μm)	8.51 ± 0.10a	8.68 ± 0.18a	7.81 ± 0.13a	8.10 ± 0.13a
Lower epidermis thickness (μm)	7.40 ± 0.10a	7.015 ± 0.13a	6.75 ± 0.09a	6.80 ± 0.14a
Leaf thickness (μm)	136.45 ± 0.67a	127.96 ± 0.83b	130.46 ± 0.64b	129.82 ± 0.83b
No. cell (10^4)	144.64 ± 4.33a	103.47 ± 1.99b	106.07 ± 2.58b	111.33 ± 1.76b
Size of cell (μm)	15.17 ± 0.21a	15.39 ± 0.31a	14.58 ± 0.15a	15.42 ± 0.30a

Data are presented as mean ± standard error. Letters indicate significant differences at p = 0.05 by Tukey's test.

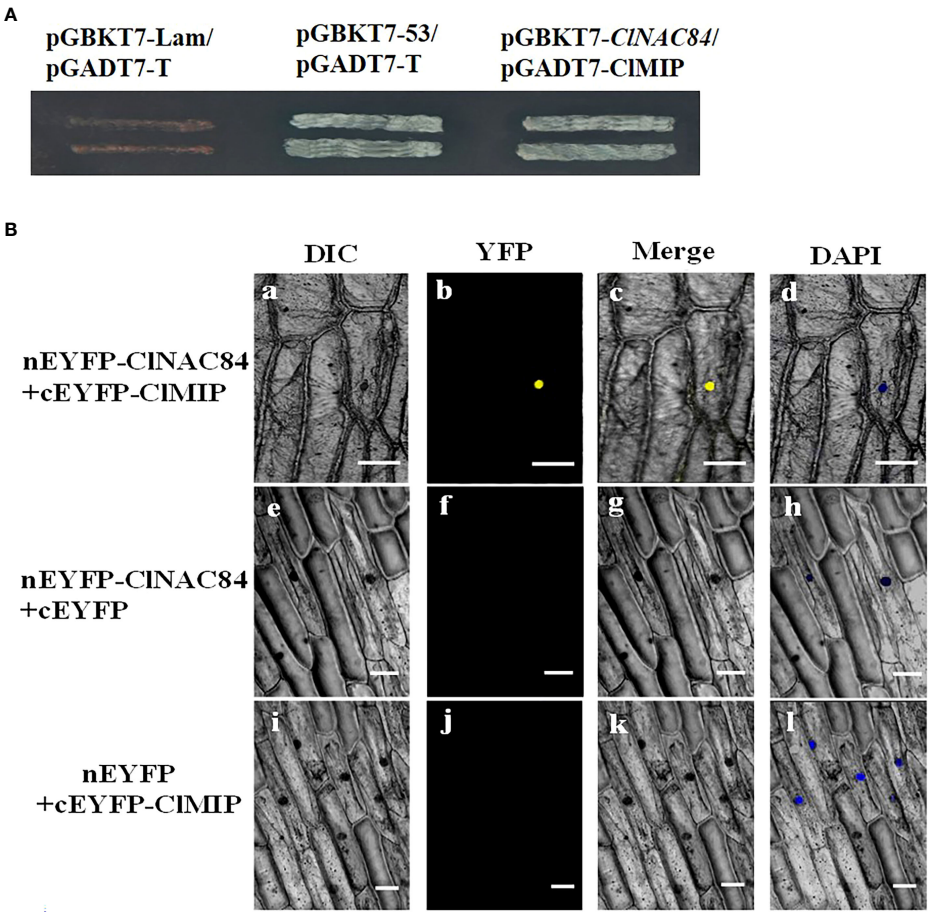

FIGURE 3
Interaction between ClNAC84 and ClMIP. **(A)** Interaction between ClNAC84 and ClMIP *in vitro* as demonstrated by yeast two-hybrid (Y2H) assay. pGBKT7-Lan/pGADT7-T and pGBKT7-53/pGADT7-T were used as negative and positive control, respectively. Selection of yeast colonies culture on SD medium lacking tryptophan, histidine, leucine, and adenine and containing X-α-Gal. **(B)** BiFC assay of ClNAC84 and ClMIP interaction in transiently transformed onion epidermal cells. Differential interference contrast (DIC), YFP fluorescence, merged images are shown for each transgenic combination and 4,6-diamidino-2-phenylindole staining (DAPI). The construct pairs of [ClNAC84-nEYFP and cEYPF] and [ClMIP-cEYFP and nEYFP] were used as negative controls. Bars = 100 mm.

Altered expression of ClKRPs in ClMIP overexpression and ClNAC84 overexpression lines

The relative expression of *ClKRPs* was analyzed in *ClMIP* and *ClNAC84* overexpression lines by qRT-PCR. The relative expression of *ClKRP5* and *ClKRP8* in the *ClMIP* overexpression lines was higher than that in WT *C. lavandulifolium*. Similarly, the relative expression of *ClKRP3*, *ClKRP4*, and *ClKRP5* was also high in *ClNAC84* overexpression lines. Therefore, the relative expression of *ClKRP5* in both *ClMIP* overexpression and *ClNAC84* overexpression lines was higher than that in WT (Figures 5A, B). This suggests that ClMIP may regulate the cell cycle through *ClKRP5*.

ClMIP proteins can activate ClKRP5 expression

To confirm whether ClMIP can bind to the *ClKRP5* promoter, we performed a yeast one-hybrid and transient expression assay using the luciferase reporter system. The pHIS-*ClKRP5pro* vector containing the *ClKRP5* promoter sequence (1479 bp) was co-transformed into yeast Y187 competent cells with an AD-ClMIP vector containing the ClMIP sequence and an empty pGADT7 vector (AD), respectively. The yeast cells of pHIS-*ClKRP5pro* and AD-*ClMIP* and pHIS-*ClKRP5pro* and AD groups grew well in the yeast medium without His, Trp, and Leu. The yeast cells containing pHIS-*ClKRP5pro* and AD-*ClMIP* grew normally,

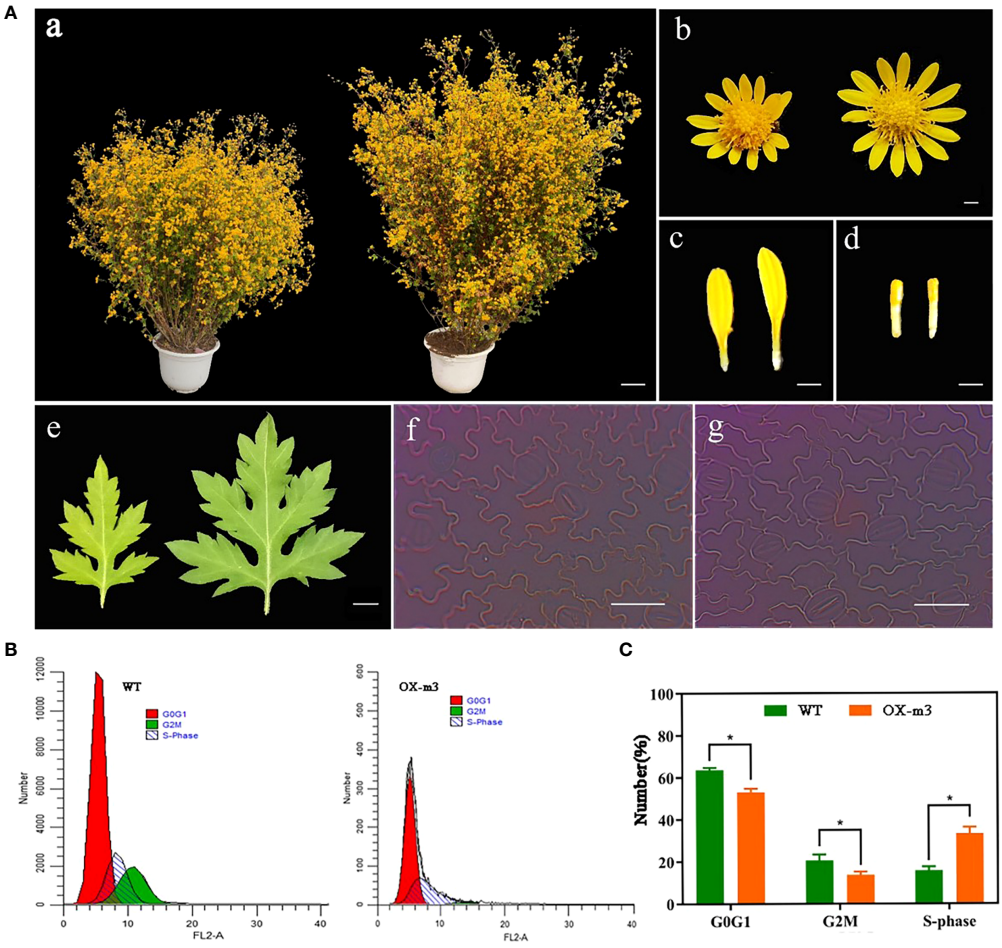

FIGURE 4
Involvement of ClMIP in the regulation of cell cycle. **(A)** Phenotypic characterization of ClMIP overexpression *C. lavandulifolium*. (a, b, c, d, and e) Plants, flowers, ligulate florets, tuber florets, and leaves of wild-type plants on the left and the overexpression line (OX-m3) on the right. a: bar = 5 cm; b, c, and d: bars = 0.2 cm; e: bar = 0.5 cm. (f and g) First layer epidermal cells of wild-type plants (f) and the overexpression line (g); bars = 50 μm. **(B)** Comparison of the flow cytometric profiles of wild-type and *ClMIP* overexpression *C. lavandulifolium*. Red peaks indicate normal G0-G1 cell number, green peaks indicate G2-M cell number, and black peaks indicate S phase cell number. **(C)** The cell number at different phases of the cell cycle. The percentages were derived from **(B)**.

but those with pHIS-*ClKRP5pro* and empty pGADT7 did not grow on yeast medium lacking His, Trp, and Leu with the addition of 50 mM 3-aminotrizole (3-AT) (Figure 6A). For the luciferase reporter system, a construct containing the *ClKRP5* promoter region fused to firefly luciferase (P_{ClKRP5}:LUC) was agroinfiltrated into tobacco (*Nicotiana benthamiana*) leaves together with *35S::ClMIP* and (or) *35S::ClNAC84*. LUC bioluminescence was induced in leaves co-infiltrated with $_{ClKRP5}$:LUC + *35S::ClMIP* + *35S::ClNAC84*, followed by co-infiltration with $_{ClKRP5}$:LUC + *35S::ClMIP*. The intensity of bioluminescence was very weak in leaves infiltrated with *P* $_{ClKRP5}$:LUC and *P* $_{ClKRP5}$:LUC + *35S::ClNAC84* (Figures 6B, C). These results indicate that ClMIP activated the transcription of *ClKRP5*.

Discussion

Involvement of ClNAC84 in the regulation of cell cycle

The NAC gene family is a plant-specific transcription factor that is widely involved in plant growth and development (Jin et al., 2017; Yan et al., 2017). NAC protein has a consensus sequence at the NAC domain, which contains 160 amino acid residues and a highly divergent sequence in the transcriptional activation or repression region located in the C-terminal. The ClNAC84 protein contains a NAC domain (a-e subdomains) but has no transcriptional activation activity (Figure 1C). The hydrophobicity associated with FVFY residue interference with

TABLE 3 Morphology of wild type and transgenic *ClMIP* over-expressing of *C. avandulifolium*.

Characters	WT	OX-m1	OX-m2	OX-m3
Plant height (cm)	71.87 ± 1.96a	57.2 ± 1.69b	60.85 ± 0.76b	62.52 ± 0.25b
Leaf length (cm)	3.82 ± 0.21a	3.13 ± 0.09b	3.33 ± 0.19b	2.90 ± 0.06b
Leaf width (cm)	2.54 ± 0.09a	1.91 ± 0.10b	1.77 ± 0.12b	1.85 ± 0.09b
Leaf area (mm^2)	391.56 ± 7.76a	277.74 ± 4.63b	256.38 ± 8.98c	259.20 ± 7.33c
Inflorescence diameter (mm)	17.49 ± 0.33a	13.60 ± 0.47b	13.96 ± 0.47b	13.58 ± 0.15b
Flower disc diameter (mm)	7.15 ± 0.28a	5.97 ± 0.21b	5.76 ± 0.23b	5.65 ± 0.23b
No. of ligulate florets	15.4 ± 0.51a	14.4 ± 1.14a	14.46 ± 0.89a	14.8 ± 0.75a
Ligulate flower length (mm)	7.29 ± 0.33a	6.89 ± 0.39a	6.75 ± 0.51a	6.93 ± 0.17a
No. of tubular florets	82.00 ± 2.58a	71.60 ± 1.56b	72.00 ± 0.22b	70.00 ± 1.58b
Tubular flower length (mm)	4.52 ± 0.28a	3.40 ± 0.08b	3.45 ± 0.18b	3.48 ± 0.21b
Cell area (μm^2)	1041.00 ± 49.24a	838.56 ± 15.58b	838.13 ± 21.75b	812.62 ± 23.11b
NO. cell ($\times 10^4$)	37.77 ± 1.47a	33.15 ± 0.76b	30.63 ± 1.25b	31.96 ± 1.35b

Data are presented as mean ± standard error. Letters indicate significant differences at p=0.05 by Tukey's test.

DNA binding may be responsible for repression (Puranik et al., 2012). Phylogenetic analysis of NAC proteins from *Arabidopsis* and rice revealed that the ClNAC84 protein belonged to the ONAC22 subgroup (Figure S4). In this novel subgroup, *ANAC36*-overexpressing transgenic plants showed a semi-dwarf phenotype in *Arabidopsis* (Hao et al., 2010). We found that *ClNAC84* overexpression lines also showed a dwarf phenotype, including the flowers, leaves, and plant height. Microscopic observation of cell size and cell number revealed that cell number reduction was the main cause of dwarfing in overexpression lines (Figure 3A).

Yeast is a model system for studying gene function. Mu et al. (2019) found that *AtMYB59* overexpressing yeast cells had two nuclei and appeared to be three times longer than the control cells. Wang et al. (2004) reported that *TaRAN1I* overexpression inhibits the cell cycle and changes the morphology of yeast cells. Here, the yeast cell cycle was blocked by *ClNAC84* overexpression, which led to two-nuclei yeast cells, further confirming that *ClNAC84* is involved in the cell cycle.

In plants, cell cycle arrest may lead to a reduction in cell numbers. The cell cycle includes four phases. The initial quiescent (G0-G1) phase is when cell cycle regulatory protein synthesis and activation begins. When the cells reach the checkpoint and activation occurs, DNA begins replication in the S-phase. After DNA replication, the cell enters the G2 and M phases and divides into two identical cells (Day et al., 1996; Ren et al., 2002; Sakaue-Sawano et al., 2008). Our data showed that cell number reduction in *ClNAC84* overexpression *C. lavandulifolium* was due to stagnation of the S and G2M phases (Figures 2B, C). The G1-to-S-phase transition is a key regulatory point in the cell cycle, which requires the concerted action of specific proteins, such as E2F, CYCD3;1, CDK, and ICK/KRP (Zhang et al., 2016). The relative expression of *ClE2F*, *ClCYCA3;1*, *ClCYCD6;1*, and *ClCKDA* in *ClNAC84* overexpression *C. lavandulifolium* was lower than that in WT, but the expression levels of *ClKRP* were higher than those in WT (Figure S5). *CYCD3;1* expression in *Arabidopsis* results in a reduced proportion of cells in the G1 phase (Dewitte et al., 2003). These results suggest that ClNAC84 is involved in the KRP pathway.

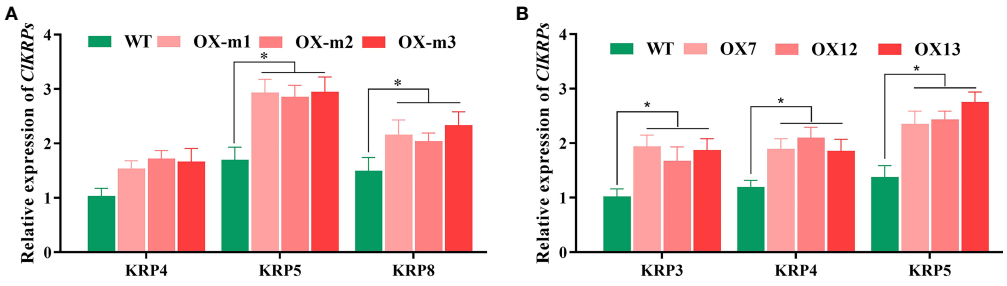

FIGURE 5
Relative expression of ClKRPs between **(A)** *ClMIP* and **(B)** *ClNAC84* overexpression *C. lavandulifolium*. * p < 0.05 levels, based on t-test.

10.3389/fhort.2022.1042105

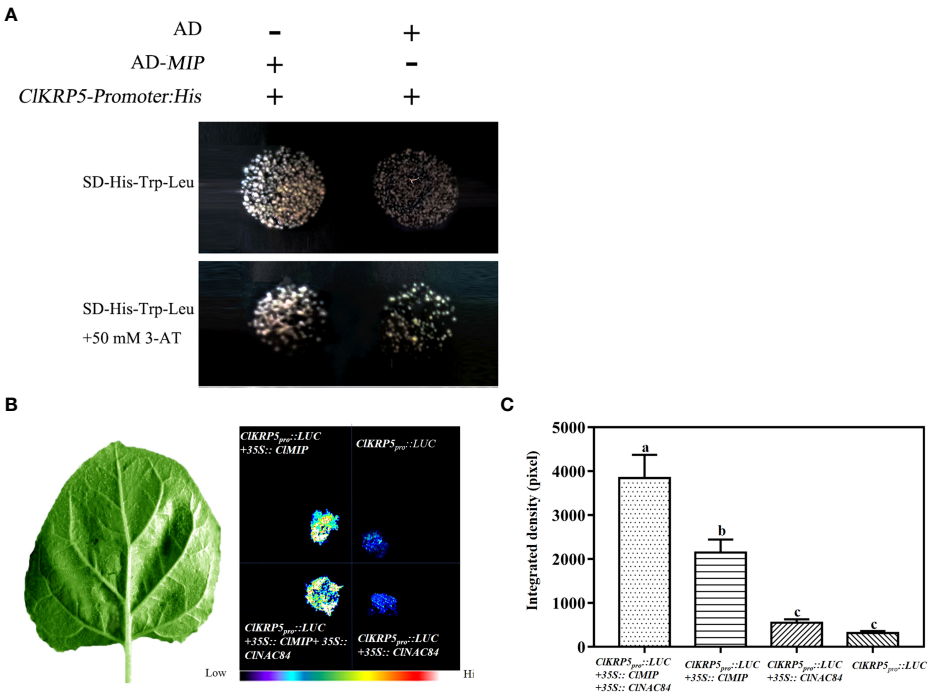

FIGURE 6
ClNAC84 interaction with ClMIP protein promotes *ClKRP5* expression. **(A)** Yeast one-hybrid assay between ClMIP protein and the promoter of *ClKRP5*. The co-transfected plasmids were cultured in yeast medium lacking His, Trp, and Leu (above) and His, Trp, and Leu with 50 mM 3-AT (below). **(B)** Representative images of transient expression assays in *Nicotiana benthamiana* leaves expressing P_{krp5}*:LUC*, P_{krp5}*:LUC +35S::ClMIP*, P_{krp5}*:LUC +35S::ClMIP + 35S::ClNAC84*, and P_{krp5}*:LUC + 35S::ClNAC84* as displayed by bright field (left) and dark field (right). **(C)** Intensities of the LUC bioluminescence presented in **(B)** measured using ImageJ analysis software. Data are shown as means + SE (n = 6). Different lowercase letters indicate significant differences ($p < 0.05$).

Involvement of ClMIP in the regulation of cell cycle

ClMIP is also known as ClAE or FAM96 (family with sequence similarity 96, member B). ClMIP contained one DUF59 (domain of unknown function 59) and a signal peptide in the N-terminal (Figure S6A). Green fluorescence of *35S::GFP-ClMIP* markedly accumulated in the onion epidermal cell nucleus (Figure S6B). The yeast assay showed that ClMIP promoted transcriptional activation in yeast cells (Figure S6C). *ClMIP* overexpression in *C. lavandulifolium* resulted in a small phenotype, which was similar to that of the *ClNAC84* overexpression plants. The number of epidermal cells was reduced in the *ClMIP* overexpression lines relative to that in WT plants (Figure 4A). *ClMIP* overexpression in *C. lavandulifolium* resulted in smaller plant stem, flowers, and

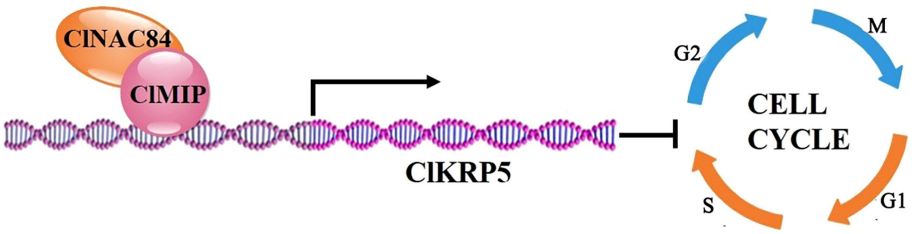

FIGURE 7
Model for *ClNAC84*, *ClMIP*, and *ClKRP5* inhibiting cell cycle. Interaction between ClNAC84 and ClMIP promotes ClKRP5 expression and inhibits cells cycling through the G0 and S phases.

leaves than those of WT plants, which were similar to those of *ClNAC84* overexpression *C. lavandulifolium*. Mip18 localized to the mitotic spindle and interacted with Ciao1, an ANT2 protein, regulating nucleotide excision repair and transcription; the siRNA-mediated knockdown of MIP18 results in improper chromosome segregation (Ito et al., 2010). The *AE7* (AS1/2 ENHANCER7) gene encodes a protein of the DUC59 superfamily, which is required for leaf polarity. The *ae7* mutant showed leaf adaxial–abaxial polarity defects (Yuan et al., 2010). Therefore, the DUF59 domain may be involved in cell division and changes in leaf morphological structure.

ClNAC84 interaction with ClMIP protein promotes ClKRP5 expression

The cell numbers of both *ClNAC84* and *ClMIP* overexpression *C. lavandulifolium* were reduced and the cell cycle was inhibited (Figure 2, Figure 4), suggesting similar genetic functions. This further indicates that ClMIP interacts with ClNAC84. Luc bioluminescence experiments showed that ClNAC84 and ClMIP bind to ClKRP5 promoter elements (Figure 6). The relative expression of *ClKPR5* was significantly increased in *ClMIP* overexpression and *ClNAC84* overexpression lines when compared to that of WT plants (Figure 5). KRP plays an important role in the cell cycle. The G2/M transition most likely requires CYCA and CYCB proteins to form CYC/CDK complexes (Churchman et al., 2006; Francis, 2011; Li et al., 2016). These complexes were also inhibited by the expression of KRPs to regulate cell cycle progression (Inze and De Veylder, 2006). The KRP family has seven members in *Arabidopsis*, which has various levels in different tissues (Cheng et al., 2013), and *KRP* overexpression in *Arabidopsis* results in some common phenotypes, such as small plant size, serrated leaves, and reduced cell number (Wang et al., 2000; Schnittger et al., 2003; Li et al., 2016).

In summary, we propose a model to describe cell cycle regulation by *ClNAC84* expression and its interaction with ClMIP protein to promote the *ClKRP5* expression to restrict the cell cycle (Figure 7).

Data availability statement

The datasets presented in this study can be found in online repositories. The names of the repository/repositories and accession number(s) can be found in the article/Supplementary Material.

Author contributions

Conceived and designed the experiments: FC. Performed the experiments: RG, HW, XQ, LZ, XY. Analyzed the data: RG, HW, XQ, LZ. Contributed reagents/materials/analysis tools: RG, HW, XQ. Wrote the paper: RG, SC, JJ, ZW, FC. All authors contributed to the article and approved the submitted version.

Funding

This work was financially supported grants from National Natural Science Foundation of China (31730081, 31872149, 32060696), Natural Science Foundation of Jiangsu Province (BK20190076), the earmarked fund for Jiangsu Agricultural Industry Technology System, and A project Funded by the Priority Academic Program Development of Jiangsu Higher Education Institutions. The foundation of Key Laboratory of Landscaping, and Ministry of Agriculture and Rural Affairs (KF201902).

Conflict of interest

The authors declare that the research was conducted in the absence of any commercial or financial relationships that could be construed as a potential conflict of interest.

Publisher's note

Supplementary material

The Supplementary Material for this article can be found online at: https://www.frontiersin.org/articles/10.3389/fhort.2022.1042105/full#supplementary-material

SUPPLEMENTARY FIGURE 1
Transcript abundance of *ClNAC84* in wild type and transgenic *C. lavandulifolium*. WT: wild type. Different numbers representing for 2#, 7#, 8#, 12#, 13# and 17# transgenic lines.

SUPPLEMENTARY FIGURE 2
ClNAC84 gene expression in pESPM-ClNAC transformants with VB1 (+VB1) or without. VB1 (−VB1) by RT-PCR analyses.

SUPPLEMENTARY FIGURE 3
Transcript abundance of *ClMIP* in wild type and transgenic *C. lavandulifolium*. WT: wild type. Different numbers representing for OX-1m, OX-2m, OX-3m transgenic lines.

SUPPLEMENTARY FIGURE 4
Unrooted phylogenetic tree of NAC between *Arabidopsis thaliana* and rice.

SUPPLEMENTARY FIGURE 5
Relative expression of genes between ClMIP and ClNAC84 overexpression *C. lavandulifolium*.

SUPPLEMENTARY FIGURE 6
Comparison of deduced amino acid sequences of ClMIP with MIPs from other plant species **(A)**, AaMIP18(PWA83908.1), CcAE7 (XP_024994445.1), HaAE7(XP_021969890.1), LsAE7(XP_023750175.1) DcAE7(GEX21963.1). Subcellular localization **(B)** and transactivation of ClMIP **(C)**.

References

Aida, M., Ishida, T., Fukaki, H., Fujisawa, H., and Tasaka, M. (1997). Genes involved in organ separation in *Arabidopsis:* an analysis of the cup-shaped cotyledon mutant. *Plant Cell* 9, 841–857. doi: 10.1105/tpc.9.6.841

Aida, M., and Tasaka, M. (2006). Genetic control of shoot organ boundaries. *Curr. Opin. Plant Biol.* 9, 72–77. doi: 10.1016/j.pbi.2005.11.011

Aida, M., Vernoux, T., Furutani, M., Traas, J., and Tasaka, M. (2002). Roles of PIN-FORMED1 and MONOPTEROS in pattern formation of the apical region of the arabidopsis embryo. *Development* 129, 3965–3974. doi: 10.1242/dev.129.17.3965

Cheng, Y., Cao, L., Wang, S., Li, Y., Shi, X., Liu, H., et al. (2013). Downregulation of multiple CDK inhibitor ICK/KRP genes upregulates the E2F pathway and increases cell proliferation, and organ and seed sizes in arabidopsis. *Plant J.* 75, 642–655. doi: 10.1111/tpj.12228

Churchman, M. L., Brown, M. L., Kato, N., Kirik, V., Hulskamp, M., Inze, D., et al. (2006). SIAMESE, a plant-specific cell cycle regulator, controls endoreplication onset in arabidopsis thaliana. *Plant Cell* 18, 3145–3157. doi: 10.1105/tpc.106.044834

Day, I. S., Reddy, A., and Golovkin, M. (1996). Isolation of a new mitotic-like cyclin from arabidopsis: complementation of a yeast cyclin mutant with a plant cyclin. *Plant Mol. Biol.* 30, 565–575. doi: 10.1007/BF00049332

Dewitte, W., Riou-Khamlichi, C., Scofield, S., Healy, J. M., Jacqmard, A., Kilby, N. J., et al. (2003). Altered cell cycle distribution, hyperplasia, and inhibited differentiation in *Arabidopsis* caused by the d-type cyclin CYCD3. *Plant Cell* 15, 79–92. doi: 10.1105/tpc.004838

Fang, Y., You, J., Xie, K., Xie, W., and Xiong, L. (2008). Systematic sequence analysis and identification of tissue-specific or stress-responsive genes of NAC transcription factor family in rice. *Mol. Genet. Genomics* 280, 547–563. doi: 10.1007/s00438-008-0386-6

Francis, D. (2011). A commentary on the G(2)/M transition of the plant cell cycle. *Ann. Botan* 107, 1065–1070. doi: 10.1093/aob/mcr055

Gao, R., Wang, H., Dong, B., Yang, X., Chen, S., Jiang, J., et al. (2016). Morphological, genome and gene expression changes in newly induced autopolyploid *Chrysanthemum lavandulifolium* (Fisch. ex trautv.) makino. *Int. J. Mol. Sci.* 17, 1690-1702. doi: 10.3390/ijms17101690

Gao, R., Yan, Y., Yang, X., Wang, Y., Fang, W., Chen, S., et al. (2018). *ClE2F1* overexpression enhances plant growth in *Chrysanthemum lavandulifolium* (Fisch. ex trautv.) makino. *Plant Mol. Biol. Rep.* 36, 341–349. doi: 10.1007/s11105-018-1084-0

Grandjean, O. (2004). *In vivo* analysis of cell division, cell growth, and differentiation at the shoot apical meristem in *Arabidopsis*. *Plant Cell* 16 (1), 74–87. doi: 10.1105/tpc.017962

Hao, Y. J., Song, Q. X., Chen, H. W., Zou, H. F., Wei, W., Kang, X. S., et al. (2010). Plant NAC-type transcription factor proteins contain a NARD domain for repression of transcriptional activation. *Planta* 232, 1033–1043. doi: 10.1007/s00425-010-1238-2

Huang, H., Wang, Y., Wang, S., Wu, X., Yang, K., Niu, Y., et al. (2012). Transcriptome-wide survey and expression analysis of stress-responsive *NAC* genes in *Chrysanthemum lavandulifolium*. *Plant Sci.* 193-194, 18–27. doi: 10.1016/j.plantsci.2012.05.004

Inze, D., and De Veylder, L. (2006). Cell cycle regulation in plant development. *Annu. Rev. Genet.* 40, 77–105. doi: 10.1146/annurev.genet.40.110405.090431

Ito, S., Tan, L. J., Andoh, D., Narita, T., Seki, M., Hirano, Y., et al. (2010). MMXD, a TFIIH-independent XPD-MMS19 protein complex involved in chromosome segregation. *Mol. Cell* 39, 632–640. doi: 10.1016/j.molcel.2010.07.029

Jin, C., Li, K. Q., Xu, X. Y., Zhang, H. P., Chen, H. X., Chen, Y. H., et al. (2017). A novel NAC transcription factor, *PbeNAC1*, of pyrus betulifolia confers cold and drought tolerance *via* interacting with *PbeDREBs* and activating the expression of stress-responsive genes. *Front. Plant Sci.* 8, 1049. doi: 10.3389/fpls.2017.01049

Kato, H., Motomura, T., Komeda, Y., Saito, T., and Kato, A. (2010). Overexpression of the *NAC* transcription factor family gene *ANAC036* results in a dwarf phenotype in *Arabidopsis thaliana*. *J. Plant Physiol.* 167, 571–577. doi: 10.1016/j.jplph.2009.11.004

Kim, Y. S., Kim, S. G., Park, J. E., Park, H. Y., Lim, M. H., Chua, N. H., et al. (2006). A membrane-bound NAC transcription factor regulates cell division in *Arabidopsis*. *Plant Cell* 18, 3132–3144. doi: 10.1105/tpc.106.043018

Li, Q., Shi, X., Ye, S., Wang, S., Chan, R., Harkness, T., et al. (2016). A short motif in *Arabidopsis* CDK inhibitor ICK1 decreases the protein level, probably through a ubiquitin-independent mechanism. *Plant J.* 87, 617–628. doi: 10.1111/tpj.13223

Li, P., Song, A., Gao, C., Wang, L., Wang, Y., Sun, J., et al. (2015). Chrysanthemum WRKY gene *CmWRKY17* negatively regulates salt stress tolerance in transgenic *chrysanthemum* and *Arabidopsis plants*. *Plant Cell Rep.* 34, 1365–1378. doi: 10.1007/s00299-015-1793-x

Menges, M., and Murray, J. A. (2002). Synchronous *Arabidopsis* suspension cultures for analysis of cell-cycle gene activity. *Plant J.* 30, 203–212. doi: 10.1046/j.1365-313X.2002.01274.x

Mu, R. L., Cao, Y. R., Liu, Y. F., Lei, G., Zou, H. F., Liao, Y., et al. (2009). An R2R3-type transcription factor gene *AtMYB59* regulates root growth and cell cycle progression in *Arabidopsis*. *Cell Res.* 19, 1291–1304. doi: 10.1038/cr.2009.83

Ooka, H., Satoh, K., Doi, K., Nagata, T., Otomo, Y., Murakami, K., et al. (2003). Comprehensive analysis of NAC family genes in *Oryza sativa* and *Arabidopsis thaliana*. *DNA Res.* 10, 239–247. doi: 10.1093/dnares/10.6.239

Puranik, S., Sahu, P. P., Srivastava, P. S., and Prasad, M. (2012). NAC proteins: regulation and role in stress tolerance. *Trends Plant Sci.* 17, 369–381. doi: 10.1016/j.tplants.2012.02.004

Ren, B., Cam, H., Takahashi, Y., Volkert, T., Terragni, J., Young, R. A., et al. (2002). E2F integrates cell cycle progression with DNA repair, replication, and G (2./M) checkpoints. *Genes Dev.* 16, 245–256. doi: 10.1101/gad.949802

Rubio-Somoza, I., Zhou, C. M., Confraria, A., Martinho, C., von Born, P., Baena-Gonzalez, E., et al. (2014). Temporal control of leaf complexity by miRNA-regulated licensing of protein complexes. *Curr. Biol.* 24, 2714–2719. doi: 10.1016/j.cub.2014.09.058

Sakaue-Sawano, A., Kurokawa, H., Morimura, T., Hanyu, A., Hama, H., Osawa, H., et al. (2008). Visualizing spatiotemporal dynamics of multicellular cell-cycle progression. *Cell* 132, 487–498. doi: 10.1016/j.cell.2007.12.033

Schnittger, A., Weinl, C., Bouyer, D., Schobinger, U., and Hulskamp, M. (2003). Misexpression of the cyclin-dependent kinase inhibitor ICK1/KRP1 in single-celled *Arabidopsis* trichomes reduces endoreduplication and cell size and induces cell death. *Plant Cell* 15, 303–315. doi: 10.1105/tpc.008342

Souer, E., Van, A. H., Kloos, D., Mol, J., and Koes, R. (1996). The no apical meristem gene of petunia is required for pattern formation in embryos and flowers and is expressed at meristem and primordia boundarie. *Cell* 85, 159–170. doi: 10.1016/S0092-8674(00)81093-4

Tang, Y., Zhao, C. Y., Tan, S. T., and Xue, H. W. (2016). Arabidopsis type II phosphatidylinositol 4-kinase PI4Kgamma5 regulates auxin biosynthesis and leaf margin development through interacting with membrane-bound transcription factor *ANAC078*. *PloS Genet.* 12, e1006252. doi: 10.1371/journal.pgen.1006252

Wang, H., Jiang, J., Chen, S., Qi, X., Peng, H., Li, P., et al. (2013). Next-generation sequencing of the *Chrysanthemum nankingense* asteraceae. transcriptome permits large-scale unigene assembly and SSR marker discovery. *PloS One* 8, e62293. doi: 10.1016/j.plantsci.2004.03.0

Wang, X., Xu, W.-Z., Xu, Y.-Y., Chong, K., Xu, Z.-H., and Xia, G.-X. (2004). Wheat RAN1, a nuclear small G protein, is involved in regulation of cell division in yeast. *Plant Sci.* 167, 1183–1190. doi: 10.1016/j.plantsci.2004.03.011

Wang, H., Zhou, Y., Gilmer, S., Whitwill, S., and Fowke, L. C. (2000). Expression of the plant cyclin-dependent kinase inhibitor ICK1 affects cell division, plant growth and morphology. *Plant J.* 24, 613–623. doi: 10.1046/j.1365-313x.2000.00899.x

Willemsen, V., Bauch, M., Bennett, T., Campilho, A., Wolkenfelt, H., Xu, J., et al. (2008). The NAC domain transcription factors *FEZ* and *SOMBRERO* control the orientation of cell division plane in *Arabidopsis* root stem cells. *Dev. Cell* 15, 913–922. doi: 10.1016/j.devcel.2008.09.019

Yan, H., Zhang, A., Ye, Y., Xu, B., Chen, J., He, X., et al. (2017). Genome-wide survey of switchgrass NACs family provides new insights into motif and structure arrangements and reveals stress-related and tissue-specific NACs. *Sci. Rep.* 7, 3056. doi: 10.1038/s41598-017-03435-z

Yuan, Z. H., Luo, D. X., Li, G. A., Yao, X. Z., Wang, H., Zeng, M. H., et al. (2010). Characterization of the *AE7* gene in *Arabidopsis* suggests that normal cell proliferation is essential for leaf polarity establishment. *Plant J.* 64, 331–342. doi: 10.1111/j.1365-313X.2010.04326.x

Zhang, W., Xie, H. Y., Ding, S. M., Xing, C. Y., Chen, A., Lai, M. C., et al. (2016). CADM1 regulates the G1/S transition and represses tumorigenicity through the Rb-E2F pathway in hepatocellular carcinoma. *Hepatob Pancreat Dis.* 15, 289–296. doi: 10.1016/S1499-3872(16)60099-1

Zhao, C., Avci, U., Grant, E. H., Haigler, C. H., and Beers, E. P. (2008). XND1, a member of the NAC domain family in *Arabidopsis thaliana*, negatively regulates lignocellulose synthesis and programmed cell death in xylem. *Plant J.* 53, 425–436. doi: 10.1111/j.1365-313X.2007.03350.x